Published in final edited form as:
ACS Med Chem Lett. 2012 January 12; 3(1): 53–57. doi:10.1021/ml200217u.

Pyrrole-Based Antitubulin Agents: Two Distinct Binding Modalities are Predicted for C-2 Analogs in the Colchicine Site

Chenxiao Da[†], **Nakul Telang**[‡], **Peter Barelli**[‡], **Xin Jia**[‡], **John T. Gupton**[‡], **Susan L. Mooberry**[§], and **Glen E. Kellogg**[*,†]

[†]Department of Medicinal Chemistry & Institute for Structural Biology and Drug Discovery, Virginia Commonwealth University, Richmond, Virginia, USA 23298-0540

[‡]Department of Chemistry, Gottwald Center for the Sciences, University of Richmond, Richmond, Virginia, USA 23173

[§]Department of Pharmacology, University of Texas Health Science Center at San Antonio, San Antonio, Texas, USA 78229-3900

Abstract

3,5-dibromo-4-(3,4-dimethoxyphenyl)-1H-pyrrole-2-carboxylic acid ethyl ester is a promising antitubulin lead agent that targets the colchicine site of tubulin. C-2 analogs were synthesized and tested for microtubule depolymerizing and antiproliferative activity. Molecular modeling studies using both GOLD docking and HINT (Hydropathic INTeraction) scoring revealed two distinct binding modes that explain the structural-activity relationships and are in accord with the structural basis of colchicine binding to tubulin. The binding mode of higher activity compounds is buried deeper in the site and overlaps well with rings A and C of colchicine, while the lower activity binding mode shows fewer critical contacts with tubulin. The model distinguishes highly active compounds from those with weaker activities and provides novel insights into the colchicine site and compound design.

Keywords

antitubulin; hydropathic interactions; docking; multi-functional pyrroles; structure-activity relationship

Microtubules are major cytoskeletal components in eukaryotic cells and participate in a variety of cell functions including maintenance of cell shape, intracellular transport, and forming mitotic spindles for segregating chromosomes during mitosis. Microtubules assemble and disassemble by a reversible process called dynamic instability involving discrete α/β tubulin heterodimers.[1] Diverse agents suppress microtubule dynamics; in rapidly dividing cells they induce mitotic arrest and initiate apoptosis.[2] Compounds that target microtubules bind at four major binding sites: the taxane and the laulimalide/peloruside A sites for microtubule-stabilizing agents, and the vinca and colchicine sites for microtubule-destabilizing agents.[2,3] Taxanes and vinca alkaloids have achieved notable success in cancer chemotherapy, but no colchicine site agents have been approved for systemic use against cancer.[4]

[*]Corresponding Author: Tel: 804-828-6452. glen.kellogg@vcu.edu.

Supporting Information. Experimental details for the synthesis and characterization of reported compounds, procedures for the assays and additional information on the computational methods utilized. This material is available free of charge via the Internet at http://pubs.acs.org.

Recent studies of one family of colchicine site agents, analogs of combretastatin A4 (CA4), have reported antivascular actions leading to the rapid collapse of tumor vasculature.[5] A number of CA4 analogs are in clinical trials refueling the search for novel colchicine site agents. Emerging drug resistance due to the expression of the βIII-tubulin isotype has compromised the clinical use of taxanes and vinca alkaloids.[6] Resistance to different types of microtubule targeting agents was recently suggested to be related to their binding sites and that βIII-tubulin mediated drug resistance might be circumvented by colchicine site agents.[7] Natural and synthetic compounds, e.g., podophyllotoxins, arylindoles, sulfonamides, 2-methoxyestradiols and flavonoids, bind within the colchicine site.[8] This structural diversity provides many possibilities for optimization and new scaffold design. The colchicine site has been characterized with X-ray crystallography by co-crystallization of the protein with DAMA-colchicine;[9] the site is at the interface between α- and β-tubulin. Complexation with other agents has documented the flexibility of this pocket.[10] To understand the structural basis for ligand binding at the colchicine site, a common pharmacophore model was built by Nguyen *et al.* based on 15 structurally diverse colchicine site inhibitors.[11]

We previously showed that **1** (3,5-dibromo-4-(3,4-dimethoxyphenyl)-1H-pyrrole-2-carboxylic acid ethyl ester, JG-03-14, Figure 1) is a potent microtubule-destabilizing agent.[12] Since **1** inhibited the binding of [3H]colchicine, and COMPARE analysis, which evaluates the similarity between two compounds with respect to the NCI 60-cell line assay,[13] showed correlation between **1** and colchicine, it is likely that **1** also binds at this site.[14] Although **1** does not structurally resemble other classes of agents, it more or less fits the previous pharmacophore model.[14] In addition, **1** and an unfocused set of analogs produced a quantitative linear QSAR relationship between IC_{50} and HINT[15] binding score.[14] This scoring model, which considers hydrophobic and polar interactions as well as entropic effects, has been shown to correlate with binding free energy for small molecule-biomacromolecular complexes.[16].

Further investigations on autophagic cell death, polyploidy, senescence and effect on endothelial cell functions for **1** suggest that it is a viable lead candidate for optimization as a new colchicine site anticancer agent.[17–19] Of particular note is that there is considerable synthetic flexibility for **1** and analogs, such that each of the 5 atoms of the pyrrole ring can be differentially probed, elaborated and optimized for SAR. Here, we report the synthesis, physical properties and microtubule inhibitory effects for C-2 analogs of **1**. Modeling studies indicate that two distinct binding modalities are required to explain the observed SAR.

In this study, we retain the 3,4-dimethoxylphenyl at C-4 and the two bromine groups at C-3 and C-5 of **1** and focus on modifications to the ester at the C-2 position of the pyrrole core. We have previously reported[17] the synthesis of **1** (JG-03-14) and have utilized a similar sequence of reactions as outlined in Scheme 1 to prepare the new analogs listed in Table 1. 3,4-Dimethoxyphenylacetic acid (**2**) was converted to the corresponding vinamidinium salt (**3**) using Vilsmeier-Haack-Arnold conditions. **3** was condensed with glycinate esters to give either pyrrole ethyl ester (**4a**) or pyrrole t-butyl ester (**4b**). **4a** was hydrolyzed with base in aqueous ethanol to produce the corresponding pyrrole acid (**5**), which served as the key building block for the majority of the analogs. The various pyrrole esters (**6a–6i**) were constructed with the appropriate alcohol, carbonyldi-imidazole, DMF and DBU. The final step involving dibromination was accomplished with dibromodimethylhydantoin in refluxing chloroform. The only exception was converting the pyrrole t-butyl ester (**4b**) directly to the corresponding dibromopyrrole (**7**) with dibromodimethylhydantoin. All reactions gave product yields in excess of 65%.

Antiproliferative activities were measured in MDA-MB-435 cancer cells using the sulforhodamine B assay and effects on cellular microtubules were evaluated in A-10 cells using immunofluorescence as previously described.[12] Results are presented in Table 1.

For this study, the SAR was analyzed with respect to the antiproliferative activities of compounds **1** and **7a–l**. Antitubulin activity generally trends with antiproliferative activity. **1** remains the most active compound (36 nM).[12] Compared to **1**, **7a** had a 17-fold decrease in activity likely due to its 1-carbon shorter ester. Similarly, the longer and bulkier alkyl substitutions *n*-propyl (**7b**) and *i*-propyl (**7c**) decreased antiproliferative activity. Larger groups, *t*-butyl (**7d**), *n*-butyl (**7e**) or *n*-hexyl (**7f**), were tolerated but with a significant activity loss of at least 36-fold. A dramatic loss was also observed for aromatic substitutions (**7g**, **7l**). The incorporation of a comparatively polar amine did not increase the activity significantly (**7h–k**), suggesting that activity drop is truly related to sterics and not solubility.

The observation that the protonated amines (**7j**, **7k**) had a further 2-fold drop in activity compared to their free base analogs (**7h**, **7i**) may be due to their weaker ability to penetrate the cell membrane. Moreover, no microtubule effects were observed up to 10 μM for the amine derivatives, suggesting that a different mechanism of action of antiproliferation might be at play. The SAR suggests that only the properly sized group would be favorable for activity and the ethyl group of **1** provides that optimum.

To rationalize the SAR from a structure-based perspective, we performed docking studies with the X-ray crystal structure of DAMA-colchicine/tubulin (pdbid: 1sa0).[9] It should be noted that the resolution of the 1sa0 structure for αβ-tubulin is poor (3.58 Å) and resulting modeling studies have a higher degree of uncertainty than in other systems. The colchicine site is mostly buried in the β-subunit surrounded by helices H7 and H8, loop T7, and strands S8 and S9. The T5 loop of the α-subunit also contributes to the pocket (see Figure 2). DAMA-colchicine occupies the pocket such that ring A fits deep within a subpocket close to H7, ring C fits into another subpocket close to T5, ring B is centered within the main pocket and the DAMA chain is pointing to the pockets entrance. For convenience, we will refer to the subpockets where rings A and C bind as sub-pockets A and C. **1** and its analogs **7a–l** were docked in the colchicine site with poses generated by the docking program GOLD,[20] and re-scored with HINT.[15,16] The compounds can be divided into two sets based on their computationally predicted binding modes (Table 1 and Figure 2). In both modes, the dimethoxyphenyl ring locates in the subpocket A, overlapping the trimethoxyphenyl ring (ring A) of DAMA-colchicine. The positions of the C-2 ester chain differ between the two modes. In mode I, the R group of the ester has “acceptable” size (i.e., **1**, **7a–c**), and fits within subpocket C and thus overlaps well with ring C of DAMA-colchicine, while in mode II, the bulkier **7d–l** R groups extend out from the main pocket towards its opening.

To illustrate the specific interactions between the ligands and site, we calculated intermolecular HINT interaction maps[21] using **1** as representing mode I binding (Figure 3A) and **7e** representing mode II (Figure 3B).

First, subpocket A, which fits the dimethoxyphenyl ring in both modes, is quite hydrophobic. In both modes, the four-carbon side chains of Leu248β and Leu255β clamp the phenyl ring in place, while deeper in the pocket other residues lock the ligands methoxys. Polar interactions also play a part as Cys241β is in proximity to these two methoxys, with distances between the cysteines sulfur and the oxygens of 3.06 Å and 3.45 Å, thus likely forming at least one hydrogen bond to support the binding. Also in both modes, there is a favorable interaction in the main pocket between the backbone oxygen of Asn258β and the ligands pyrrole nitrogen.

Both hydrophobic and polar residues characterize sub-pocket C, which fits the esters in mode I binding. The alkyl ends reach the hydrophobic bottom, while the carboxyl oxygens anchor the ester by forming hydrogen bonds with the backbone nitrogen of Val181α. The main pocket includes its funnel opening and is much more spacious than subpocket C. It easily tolerates the size of the longer esters binding with mode II by flipping the pyrrole core - thus exposing the ester tail to the solvent while keeping the dimethoxylphenyl ring in subpocket A. Our models suggest that a new hydrogen bond, stabilizing the ester tail in mode II, is formed between the amide nitrogen of Asn101α and the ligands carbonyl oxygen. The interactions for the various R groups of **7d–l** are poorly defined as the pocket entrance broadens and has a large solvent exposure.

The compounds in mode I displayed notably higher antiproliferative activity and antitubulin activity than the compounds in mode II. It is clearly important to effectively occupy both subpockets A and C in the colchicine site. The SAR within the mode I set is size related: the methyl of **7a**, *n*-propyl of **7b** and the *i*-propyl of **7c** may not position the ester carbonyl (hydrogen bonded to Val181β) as well as the ethyl of **1**. In contrast, in the mode II set, the ester R extends from the pocket into (and possibly out of) the pockets entrance. The SAR simply may not be interpret-able as these tails are highly flexible and thus subject to interactions with a wide array of residues as well as solvent.

It is also instructive to compare, in detail, the binding of colchicine and the pyrrole-based compounds **1** and **7a–l**: 1) depletion of ring B of colchicine retains activity, while rings A and C, which adopt a similar conformation as in mode I, are necessary for high affinity binding;[22] 2) residues Cys241β (subpocket A) and Val181α (subpocket C) appear to be important for antitubulin activity since the removal of any A ring methoxy group close to Cys241β weakens the binding to tubulin and microtubule inhibition.[23] Also, isocolchicine, whose structural difference to colchicine is in the C ring (methoxy at C-9 and keto at C-10) binds weakly and only poorly inhibits microtubule assembly,[24] probably because of a loss of hydrogen bonding to Val181α. Both residues anchor the ligand in the more active mode I, while only Cys241β does so in the less active mode II. This may largely explain the difference in activity between the binding modes.

The HINT scores of Table 1 were poor in distinguishing between binding in mode I and II. The reasons for this failure are instructive. First, the poor resolution of the tubulin crystal structure and the flexibility of the pocket,[10] especially the T5 and T7 loops, are a partial explanation. However, the binding modes themselves and the nature of the pocket are larger factors. Table 2 lists the HINT scores in terms of two fragments - the common dimethoxyphenyl plus pyrrole (ring) and the ester. Interaction types further differentiate the latter. The total ring score is largely invariant (580±70), excluding **7b** and **7c**, where it is lower by > 200. The esters H_{HH} for mode I (750±130) is much higher than for mode II (280±90). Interestingly, H_{HH} is highest for **7b** and **7c**, but accommodation of these longer esters was penalized by poorer ring interactions. For **1** and **7a–c**, hydrophobic binding quality in subpocket C is key. Although the esters of mode II compounds appear to make productive contacts, these are in the very open funnel-like entrance of the pocket where dynamic solvent effects that can disrupt polar interactions must be assumed.

In summary, mode I is a new binding motif observed for pyrrole compounds based on JG-03-14 (**1**) that is different from previously reported binding modes.[11,14] The ester chain in mode I overlaps with the C-10 substituents of colchicine and the SAR of colchicine C-10 analogs also shows that increasing length of the alkyl chain causes a concomitant decrease in activity.[25] We propose that the deeper burial of mode I ligands is more disruptive to the association of α- and β-tubulin subunits than is binding with mode II. We are continuing

design and development of additional JG-03-14 (**1**) analogs by focusing on other positions of the pyrrole core as we attempt to gain a full view of the SAR.

Supplementary Material

Refer to Web version on PubMed Central for supplementary material.

Acknowledgments

Funding Sources

This work was partially supported by NIH R01 CA135043 (to D.A. Gewirtz, VCU), NIH R15 CA067236 (to J.T.G.) and the Presidents Council Research Excellence Award (to S.L.M).

The excellent technical assistance of Ms. Lyda Robb, Ms. Cara Westbrook and Mr. Nicholas Dbydal-Hargreaves is gratefully acknowledged.

References

1. Jordan MA, Wilson L. Microtubules as a Target for Anticancer Drugs. Nat Rev Cancer. 2004; 4:253–265. [PubMed: 15057285]
2. Dumontet C, Jordan MA. Microtubule-Binding Agents: A Dynamic Field of Cancer Therapeutics. Nat Rev Drug Discovery. 2010; 9:790–803.
3. Bennett MJ, Barakat K, Huzil JT, Tuszynski J, Schriemer DC. Discovery and Characterization of the Laulimalide-Microtubule Binding Mode by Mass Shift Perturbation Mapping. Chem Biol. 2010; 17:725–734. [PubMed: 20659685]
4. Stanton RA, Gernert KM, Nettles JH, Aneja R. Drugs That Target Dynamic Microtubules: A New Molecular Perspective. Med Res Rev. 2011; 31:443–481. [PubMed: 21381049]
5. Siemann DW. The Unique Characteristics of Tumor Vasculature and Preclinical Evidence for Its Selective Disruption by Tumor-Vascular Disrupting Agents. Cancer Treat Rev. 2011; 37:63–74. [PubMed: 20570444]
6. Seve P, Dumontet C. Is Class III Beta-tubulin a Predictive Factor in Patients Receiving Tubulin-binding Agents? Lancet Oncol. 2008; 9:168–175. [PubMed: 18237851]
7. Stengel C, Newman SP, Leese MP, Potter BV, Reed MJ, Purohit A. Class III Beta-tubulin Expression and in vitro Resistance to Microtubule Targeting Agents. Br J Cancer. 2010; 102:316–324. [PubMed: 20029418]
8. Chen J, Liu T, Dong X, Hu Y. Recent Development and SAR Analysis of Colchicine Binding Site Inhibitors. Mini-Rev Med Chem. 2009; 9:1174–1190. [PubMed: 19817710]
9. Ravelli RB, Gigant B, Curmi PA, Jourdain I, Lachkar S, Sobel A, Knossow M. Insight into Tubulin Regulation from a Complex with Colchicine and a Stathmin-like Domain. Nature. 2004; 428:198–202. [PubMed: 15014504]
10. Dorleans A, Gigant B, Ravelli RB, Mailliet P, Mikol V, Knossow M. Variations in the Colchicines-binding Domain Provide Insight into Structural Switch of Tubulin. Proc Natl Acad Sci U S A. 2009; 106:13775–13779. [PubMed: 19666559]
11. Nguyen TL, McGrath C, Hermone AR, Burnett JC, Zaharevitz DW, Day BW, Wipf P, Hamel E, Gussio R. A Common Pharmacophore for a Diverse Set of Colchicine Site Inhibitors Using a Structure-Based Approach. J Med Chem. 2005; 48:6107–6116. [PubMed: 16162011]
12. Mooberry SL, Weiderhold KN, Dakshanamurthy S, Hamel E, Banner EJ, Kharlamova A, Hempel J, Gup-ton JT, Brown ML. Identification and Characterization of a New Tubulin-Binding Tetrasubstituted Brominated Pyrrole. Mol Pharmacol. 2007; 72:132–140. [PubMed: 17456786]
13. Cleaveland ES, Monks A, Vaigro-Wolff A, Zaharevitz DW, Paull K, Ardalan K, Cooney DA, Ford H Jr. Site of Action of Two Novel Pyrimidine Biosynthesis Inhibitors Accurately Predicted by the COMPARE Program. Biochem Pharmacol. 1995; 49:947–954. [PubMed: 7741767]

14. Tripathi A, Fornabaio M, Kellogg GE, Gupton JT, Gewirtz DA, Yeudall WA, Vega NE, Mooberry SL. Docking and Hydrophobic Scoring of Polysubstituted Pyrrole Compounds with Antitubulin Activity. Bioorg Med Chem. 2008; 16:2235–2242. [PubMed: 18083520]
15. Kellogg EG, Abraham DJ. Hydrophobicity: Is LogPo/w More than the Sum of Its Parts? Eur J Med Chem. 2000; 35:651–661. [PubMed: 10960181]
16. Spyrakis F, Amadasi A, Fornabaio M, Abraham DJ, Mozzarelli A, Kellogg GE, Cozzini P. The Consequences of Scoring Docked Ligand Conformations using Free Energy Correlations. Eur J Med Chem. 2007; 42:921–933. [PubMed: 17346861]
17. Gupton J, Burnham B, Krumpe K, Du K, Sikorski J, Warren A, Barnes C, Hall I. Synthesis and Cytotoxicity of 2,4-Disubstituted and 2,3,4-Trisubstituted Brominated Pyrroles in Murine and Human Cultured Tumor Cells. Arch Pharm Pharm Med Chem. 2000; 333:3–9.
18. Dalyot-Herman N, Delgado-Lopez F, Gewirtz DA, Gupton JT, Schwartz EL. Interference with Endothelial Cell Function by JG-03-14, An Agent that Binds to the Colchicine Site on Microtubules. Biochem Pharmacol. 2009; 78:1167–1177. [PubMed: 19576183]
19. Arthur CR, Gupton JT, Kellogg GE, Yeudall WA, Cabot MC, Newsham IF, Gewirtz DA. Autophagic Cell Death, Polyploidy and Senescence Induced in Breast Tumor Cells by the Substituted Pyrrole JG-03-14, a Novel Microtubule Posion. Biochem Pharmacol. 2007; 74:981–991. [PubMed: 17692290]
20. Jones G, Willett P, Glen R. Molecular Recognition of Receptor Sites Using a Genetic Algorithm with a Description of Desolvation. J Mol Biol. 1995; 245:43–53. [PubMed: 7823319]
21. Wireko FC, Kellogg GE, Abraham DJ. Allosteric Modifiers of Hemoglobin. 2. Crystallographically Determined Binding Sites and Hydrophobic Binding/Interaction Analysis of Novel Hemoglobin Oxygen Effectors. J Med Chem. 1991; 34:758–767. [PubMed: 1995898]
22. Bhattacharyya B, Panda D, Gupta S, Banerjee M. Anti-Mitotic Activity of Colchicine and the Structural Basis for Its Interaction with Tubulin. Med Res Rev. 2008; 28:155–183. [PubMed: 17464966]
23. Andreu JM, Perez-Ramirez B, Gorbunoff MJ, Ayala D, Timasheff SN. Role of the Colchicine Ring A and Its Methoxy Groups in the Binding to Tubulin and Microtubule Inhibition. Biochemistry. 1998; 37:8356–8368. [PubMed: 9622487]
24. Hastie SB, Williams RC Jr, Puett D, Macdonald TL. The Binding of Isocolchicine to Tubulin. Mechanisms of Ligand Association with Tubulin. J Biol Chem. 1989; 264:6682–6688. [PubMed: 2708333]
25. Staretz ME, Hastie SB. Synthesis and Tubulin Binding of Novel C-10 Analogues of Colchicine. J Med Chem. 1993; 36:758–764. [PubMed: 8459402]

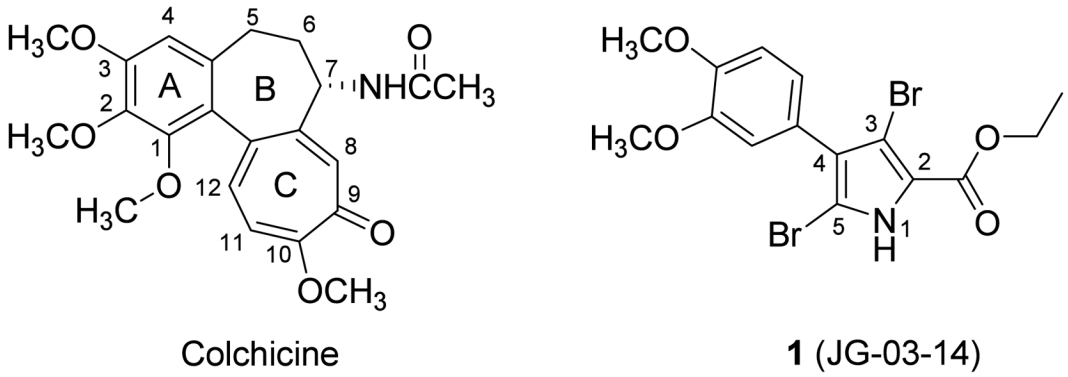

Figure 1.
Structures of colchicine and lead compound JG-03-14(**1**).

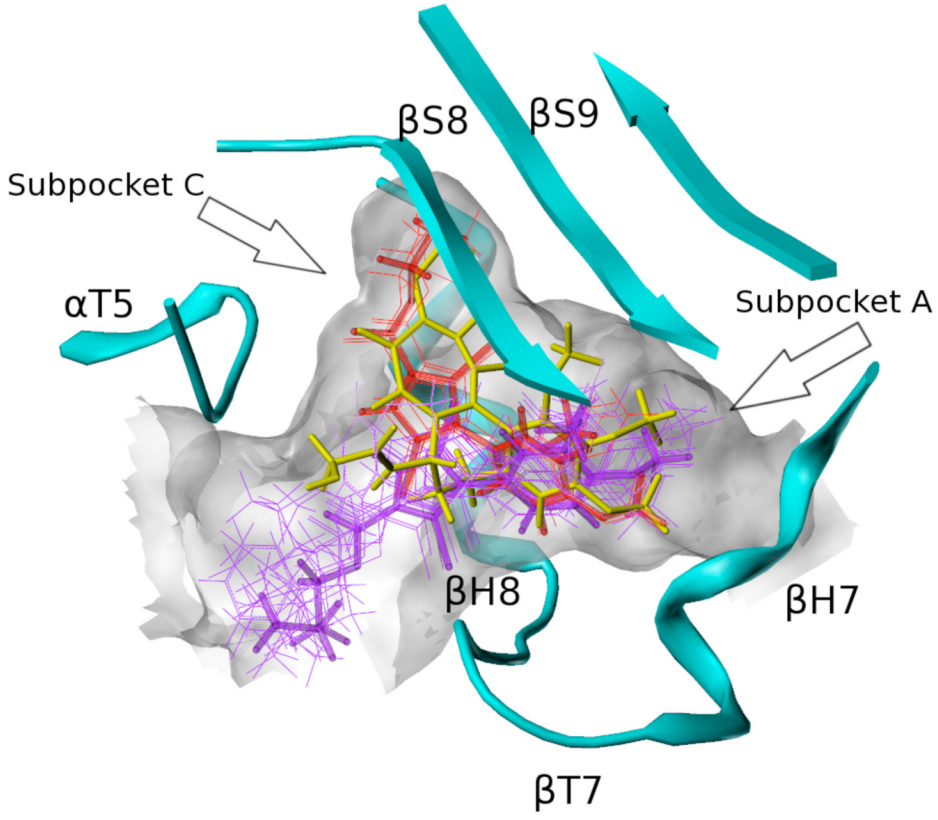

Figure 2.
Colchicine (yellow) and binding modes of pyrrole-based C-2 analogs (mode I: red; mode II: purple). The extents of the colchicine site, as illustrated by MOLCAD, are shown in grayish white.

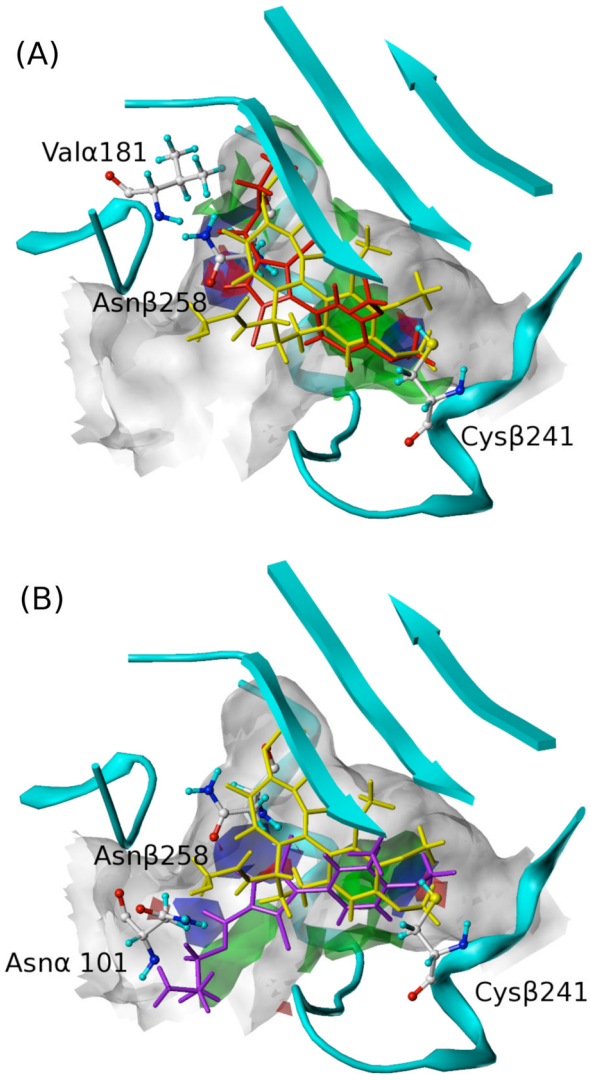

Figure 3.
HINT interaction maps of (A) **1** (binding mode I) and (B) **7e** (binding mode II). For **1** and **7e**, green contours represent favorable hydrophobic interactions; blue contours represent favorable polar interactions (hydrogen bonds, acid/base, Coulombic); red contours represent unfavorable polar interactions. **1** is shown in red, **7e** in purple and colchicine in yellow.

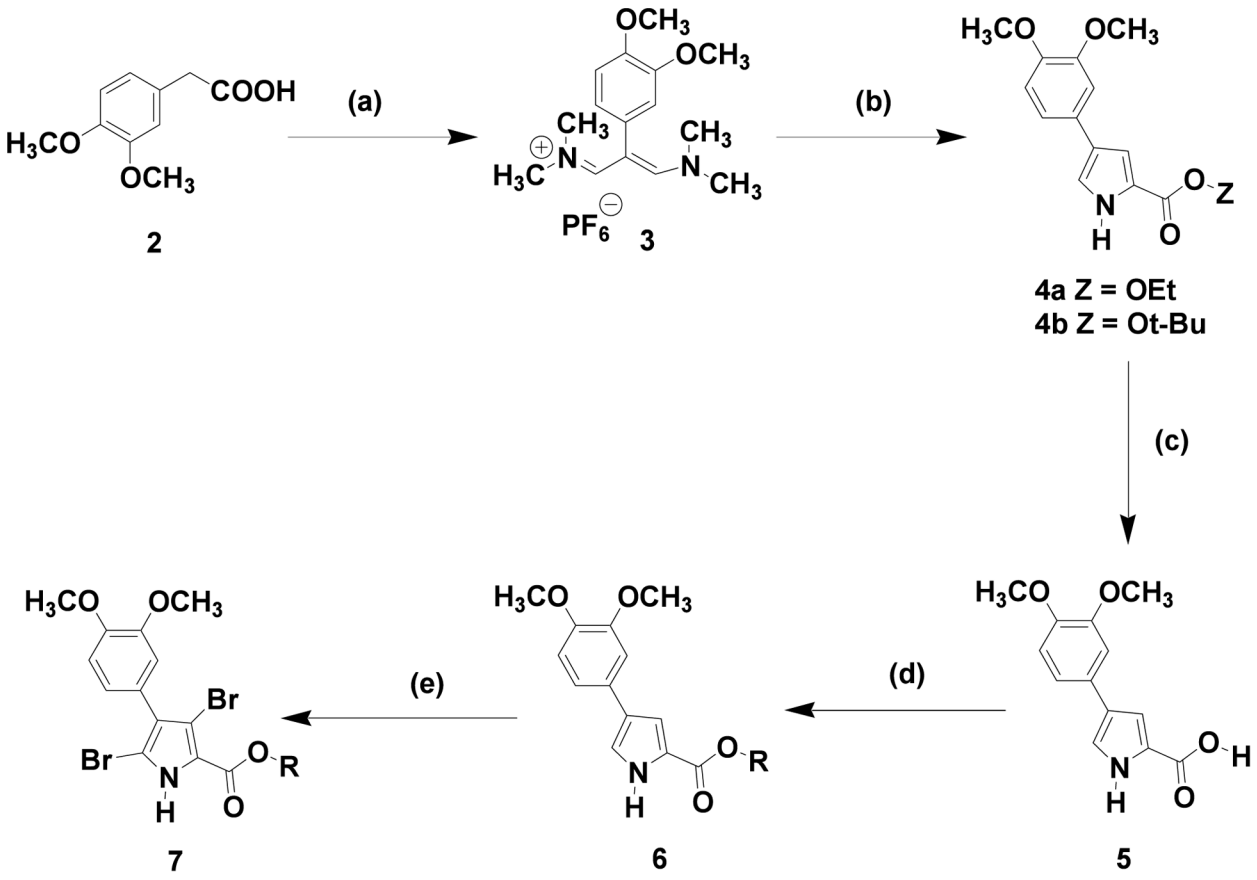

Scheme 1.

Preparation of JG-03-14 analogs with modifications at the C-2 Position; see Table 1 for identities of various R groups. Reagents: (a) $POCl_3$, DMF and heat, followed by H_2O/$NaPF_6$; (b) glycine ethyl ester or glycine *t*-butyl ester and NaO*t*-Bu, DMF and heat; (c) NaOH, EtOH/H_2O and heat; (d) ROH, 1,1′-carbonyldiimidazole, DBU and DMF; (e) dibromodimethylhydantoin, $CHCl_3$ and heat.

Table 1

Structures, biological activity and properties of pyrrole compounds 1 and 7a–l

Cmpd	R	Antiproliferation[a] IC50 (μM)	Cellular microtubule loss[b]	Binding Mode	HINT score[c]	HINT logP	ALOGPs[d]
Colchicine	-	0.016 ± 0.002	100% loss at 0.5 μM	-	549	3.24	1.59
1	ethyl	0.036 ± 0.002[e]	100% loss at 0.5 μM	I	418	2.60	4.44
7a	methyl	0.618 ± 0.07	50% loss at 5 μM	I	524	2.06	3.87
7b	*n*-propyl	0.067 ± 0.002	75% loss at 5 μM	I	157	3.14	4.74
7c	*i*-propyl	0.109 ± 0.008	70% loss at 5 μM	I	−179	3.14	4.70
7d	*t*-butyl	1.82 ± 0.3	No loss up to 10 μM	II	187	3.24	5.02
7e	*n* -butyl	1.30 ± 0.04	15% loss at 10 μM	II	530	3.68	5.05
7f	*n*-hexyl	3.3 ± 0.3	35% loss at 10 μM	II	256	4.76	5.83
7g	benzyl	5.3 ± 0.3	No loss up to 10 μM	II	713	3.61	5.39
7h	$-(CH_2)_3NMe_2$	4.6 ± 0.2	10% loss at 10 μM	II	293	2.52	4.10
7i	$-(CH_2)_2NMe_2$	5.2 ± 0.3	10% loss at 10 μM	II	358	2.57	3.82
7j	$-(CH_2)_3NMe_2H^+Cl^-$	8.0 ±0.3	No loss up to 10 μM	II	631	0.27	0.39
7k	$-(CH_2)_2NMe_2H^+Cl^-$	10.7 ±0.4	No loss up to 10 μM	II	774	0.78	0.27
7l	4-methoxylphenyl	18.3 ±2.7	No loss up to 10 μM	II	957	4.37	5.48

[a] Experiments were performed using human MDA-MB-435 cancer cells;

[b] Loss of interphase microtubules was evaluated in A-10 cells;

[c] 515 HINT score units ≈ 1 kcal mol^{-1} (Ref 15);

[d] ALOGPs was calculated at Virtual Computational Chemistry Laboratory, http://www.vcclab.org

[e] Ref 12.

Table 2

HINT scores by fragment and interaction type

Cmpd	Mode	HINT score[a]				
		Ring	Ester			
		H_{TOTAL}	$H_{HB} + H_{AB}$	H_{HH}	$H_{AA} + H_{BB}$	H_{HP}
1	I	492	858	711	−499	−1328
7a	I	518	680	583	−427	−1048
7b	I	363	1069	855	−593	−1681
7c	I	321	766	833	−478	−1821
7d	II	570	778	226	−398	−1169
7e	II	626	781	225	−364	−1015
7f	II	435	665	387	−369	−1046
7g	II	589	812	284	−341	−868
7h	II	557	549	268	−336	−1071
7i	II	581	726	237	−400	−1027
7j	II	650	375	213	−236	−634
7k	II	596	847	196	−403	−755
7l	II	587	827	494	−240	−924

[a] Interaction types: favorable polar (hydrogen-bond, H_{HB}, and acid/base, H_{AB}), hydrophobic (H_{HH}), unfavorable polar (acid/acid, H_{AA}, and base/base, H_{AB}) and unfavorable hydro-phobic-polar (H_{HP}).